



Hydrotropic oligomer-conjugated glycol chitosan as a carrier of paclitaxel: Synthesis, characterization, and *in vivo* biodistribution

G. Saravanakumar^a, Kyung Hyun Min^{b,c}, Dong Sik Min^{b,c}, Ah Young Kim^{b,c}, Chang-Moon Lee^d, Yong Woo Cho^d, Sang Cheon Lee^e, Kwangmeyung Kim^c, Seo Young Jeong^b, Kinam Park^f, Jae Hyung Park^{a,b,*}, Ick Chan Kwon^{c,*}

^a Department of Advanced Polymer and Fiber Materials, Kyung Hee University, Gyeonggi-do 446-701, Republic of Korea

^b Department of Life and Nanopharmaceutical Sciences, Kyung Hee University, Seoul 130-701, Republic of Korea

^c Biomedical Research Center, Korea Institute of Science and Technology, Seoul 136-791, Republic of Korea

^d Department of Chemical Engineering, Hanyang University, Ansan, Gyeonggi-do 426-791, Republic of Korea

^e Department of Oral Biology and Institute of Oral Biology, School of Dentistry, Kyung Hee University, Seoul 130-701, Republic of Korea

^f Departments of Pharmaceutics and Biomedical Engineering, Purdue University, IN 47907, USA

ARTICLE INFO

Article history:

Received 25 February 2009

Accepted 16 June 2009

Available online 26 June 2009

Keywords:

Hydrotropic oligomer

Glycol chitosan

Self-assembled nanoparticles

Paclitaxel

Cancer therapy

ABSTRACT

Development of successful formulations for poorly water-soluble drugs remains a longstanding critical and challenging issue in cancer therapy. As a potential drug carrier of paclitaxel, hydrotropic oligomer-glycol chitosan (HO-GC) was synthesized by chemical conjugation of the N,N-diethylnicotinamide-based oligomer, uniquely designed for enhancing the aqueous solubility of paclitaxel, to the backbone of glycol chitosan. Owing to its amphiphilicity, the conjugate formed self-assembled nanoparticles with a mean diameter of 313 ± 13 nm in a phosphate-buffered saline (PBS, pH 7.4 at 37 °C). HO-GC nanoparticles maintained their structure for up to 50 days in PBS. They could encapsulate a high quantity (20 wt.%) of paclitaxel (PTX) with a maximum drug-loading efficiency of 97%, due to the presence of hydrotropic inner cores. When HO-GC-PTX particles were exposed to the 0.1 M sodium salicylate solution in PBS (pH 7.4), PTX was released from nanoparticles in a sustained manner. From the cytotoxicity test, it was confirmed that HO-GC-PTX nanoparticles showed lower cytotoxicity than free PTX formulation in 50%/50% Cremophor EL/ethanol mixture. The optical imaging results indicated that near-infrared fluorescence dye (Cy5.5)-labeled HO-GC-PTX showed an excellent tumor specificity in SCC7 tumor-bearing mice, due to the enhanced permeation and retention effect. Overall, HO-GC-PTX nanoparticles might be a promising carrier for PTX delivery in cancer therapy.

© 2009 Elsevier B.V. All rights reserved.

1. Introduction

Many anticancer drugs with potent bioactivity exhibit high lipophilicity and extremely limited water solubility because they are often composed of the hydrophobic components. Hence, formulation for such hydrophobic drugs remains a longstanding critical and challenging issue in cancer therapy [1]. Paclitaxel (PTX), a potent promoter of microtubulin polymerization (causing cell death by disrupting the dynamics of cell divisions), is considered as one of the effective drugs for treatment of several solid tumor malignancies [2,3]. However, clinical applications of PTX have been hampered by its extremely poor water solubility (less than 1 µg/mL) [4]. Although PTX

is currently used by dissolving it in a 50/50 (V/V) mixture of Cremophor EL (polyoxyethylated castor oil)/absolute ethanol, this formulation is known to induce severe side effects such as neurotoxicity, nephrotoxicity and hypersensitivity, in up to 30% of the patients [5–7]. To circumvent this problem, significant efforts have been devoted to the development of alternative formulations without the use of organic solvents and other harmful excipients. The representative strategies for improving water solubility of PTX include its conjugation to hydrophilic compounds, complex formation with cyclodextrin, and its encapsulation into nanoparticles (e.g., liposomes and polymeric micelles) [8–12].

Hydrotropic agents are water-soluble compounds that, at their high concentrations, enhance the water solubility of sparingly soluble solutes [13]. Nicotinamide and its derivatives have recently gained attention because of its effect on solubility enhancement of poorly water-soluble drugs [14]. Of various nicotinamide derivatives, N,N-diethylnicotinamide (DENA) is considered as the most effective hydrotropic agent which can increase the aqueous solubility of PTX to 39 mg/mL at a

* Corresponding authors. Kwon is to be contacted at Biomedical Research Center, Korea Institute of Science and Technology, Seoul 136-791, Republic of Korea. Park, Department of Advanced Polymer and Fiber Materials, Kyung Hee University, Gyeonggi-do 446-701, Republic of Korea.

E-mail address: ikwon@kist.re.kr (I.C. Kwon).

concentration of 3.5 M [15]. In previous studies, we reported a new hydrotropic polymer micelles of poly(ethylene glycol)-poly(2-(4-vinylbenzyloxy)-N,N-diethylnicotinamide), (PEG-PDENA), as a drug delivery carrier for PTX [16,17]. Of note, the hydrotropic polymer micelles have shown good stability with an excellent loading capacity of PTX up to 37.4 wt.% that is 3, 4-fold higher than other polymeric micelles or polymeric nanoparticles. Therefore, introducing hydrotropic polymers as hydrophobic cores in the self-assembled nanoparticles may increase the loading capacity of poorly water-soluble drugs with enhanced physical stability in aqueous conditions.

Herein, we have attempted to prepare hydrotropic DENA oligomer-conjugated glycol chitosan (HO-GC) nanoparticles which can imbibe a quantity of PTX and show high stability in an aqueous media. It has been demonstrated that glycol chitosan-based nanoparticles show a prolonged blood circulation *in vivo* and a high tumor specificity for delivery of hydrophobic anticancer drugs [10,18–21], peptide [22,23], and genes [24]. To produce PTX-loaded HO-GC (HO-GC-PTX) nanoparticles, we encapsulated PTX into the HO-GC nanoparticles by a simple dialysis method. In order to evaluate characteristics of HO-GC-PTX, drug release profile, cell compatibility and cellular uptake behaviors were studied, compared to free PTX and PTX-loaded hydrophobically modified glycol chitosan (HGC-PTX) nanoparticles without hydrotropic oligomers. In addition, Cy5.5-labeled HO-GC-PTX nanoparticles were intravenously injected into the SCC7 tumor-bearing mice and the tumor specificity was evaluated using *in vivo/ex vivo* optical imaging techniques in live animals.

2. Materials and methods

2.1. Materials

Glycol chitosan (MW = 2.5×10^5 , degree of deacetylation = 82.7%), [1-ethyl-3-(dimethylamino)propyl]carbodiimide hydrochloride (EDAC), 4-vinylbenzyl chloride, 2-hydroxynicotinic acid, diethylamine, 3-mercaptopropionic acid (MPA), and anhydrous N,N-dimethylformamide were purchased from Sigma-Aldrich (St. Louis, MO). 1-Hydroxybenzotriazole (HOBt) was received from TCI (Tokyo, Japan). Paclitaxel was obtained from Samyang Genex Co. (Daejeon, Korea). N,N-Azobisisobutyronitrile (AIBN), purchased from Sigma-Aldrich, was purified by recrystallization in methanol. All other reagents used in the experiments were analytical grade and used as received. Water used in all the experiments was obtained by AquaMax-ultra water purification system. 2-(4-(vinylbenzyloxy)-N,N-diethylnicotinamide) (VBODENA) monomer was prepared as reported previously [16,17].

2.2. Synthesis of the HO-GC conjugate

Hydrotropic DENA oligomer, Oligo(VBODENA)-COOH, was synthesized by free radical chain transfer polymerization of VBODENA using MPA as a chain transfer agent and AIBN as an initiator, as shown in Fig. 1. VBODENA monomer was dissolved in DMF, to which MPA and AIBN were added under nitrogen. The solution was bubbled with nitrogen, followed by three freeze-pump thaw cycles to remove oxygen. The flask was then transferred to a pre-heated oil bath maintained at 75 °C. After 15 h, the product was obtained by precipitation in diethyl ether.

HO-GC conjugate was synthesized by chemical conjugation of GC with Oligo(VBODENA)-COOH in the presence of EDAC and HOBt. In a typical reaction, GC (100 mg) was dissolved in distilled water (5 mL), and Oligo(VBODENA)-COOH (67.03 mg) dissolved in methanol (5 mL) was added under stirring. The chemical modification was initiated by adding equal amounts [1.5 equiv/Oligo(VBODENA)-COOH] of EDAC and HOBt. Thereafter, the reaction was allowed to proceed for 24 h at room temperature. The solution was then extensively dialyzed using a membrane tube (MW cutoff = 12,000–14,000; Spectrum®, Rancho

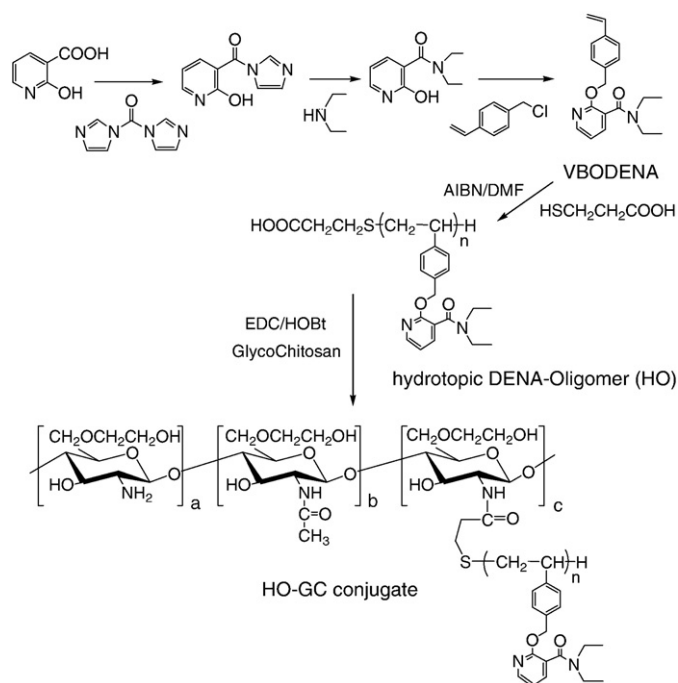


Fig. 1. Schematic representation of the synthetic route for the hydrotropic DENA oligomer-glycol chitosan (HO-GC) conjugate.

Dominquez, CA) against excess amount of water/methanol (1:4, v/v), followed by lyophilization. The chemical structure of HO and HO-GC conjugate was characterized using ^1H NMR spectra (UnityPlus 300, Varian) (see Supplementary information). As a control drug carrier, the HGC was synthesized by chemical conjugation of 5 β -cholanic acid to the backbone of GC [18–20,25]. Under optimized condition, amphiphilic HGC conjugate contained 160 molecules of 5 β -cholanic acids per glycol chitosan polymer, which formed a stable nanoparticle structure with an average diameter of 250 ± 10 nm in aqueous conditions. For cellular or animal imaging tests, 11 ± 2 of hydroxysuccinimide Cy5.5 were conjugated to HGC and HO-GC conjugates.

2.3. Preparation of PTX-loaded HO-GC (HO-GC-PTX) nanoparticles

HGC-PTX and HO-GC-PTX nanoparticles were prepared by a simple dialysis method [10]. HGC conjugates or HO-GC conjugates (100 mg) were dissolved in 4 mL of distilled water/methanol (1:1, v/v) solution. To this solution, predetermined amount of PTX (10–40 mg) in 2 mL of methanol was added. The resulting mixture was dialyzed for 2 days against distilled water using a dialysis tube (MW cutoff = 12,000–14,000). The mixture was then centrifuged at $10,000 \times g$ for 30 min to remove the unloaded PTX, followed by lyophilization. The loading efficiency of PTX in the nanoparticles was measured using the high performance liquid chromatography (HPLC, Agilent Technologies, Wilmington, DE). The mobile phase, consisting of acetonitrile/water (45:55, v/v) co-solvent, was delivered at a flow rate of 1.0 mL/min. Eluted compounds were detected at 227 nm using a Spectra 100 UV-Vis detector [16].

To test the stability of HGC-PTX and HO-GC-PTX nanoparticles in PBS, each lyophilized sample (100 mg) was dissolved in PBS (2 mg/mL), followed by sonication at 90 W for 2 min (Sigma High Intensity Ultrasonic Processor, GEX-600). Each solution was then stored at 37 °C and the images of dispersed or precipitated particles were observed according to incubation time. Furthermore, sonicated solutions were immediately centrifuged at 500, 700, and 1000 rpm for 10 min, respectively and then the characteristics of dispersed or precipitated particles were observed.

2.4. Characterizations of HO-GC and HO-GC-PTX nanoparticles

The mean diameter and size distribution of HO-GC and HO-GC-PTX nanoparticles were measured by dynamic light scattering (DLS) using a model 127-35 laser (Spectra Physics, Mountain View, CA) operated at 663 nm and 25 °C. The scattered light was measured at an angle of 90 ° with a BI-9000 AT digital autocorrelator (Brookhaven, NY). The sample concentration was kept at 1 mg/mL in PBS. The morphology of nanoparticles was observed using a transmission electron microscope (TEM, CM 200 electron microscope, Philips, CA). For sample preparation, a drop of sample solution (1 mg/mL in distilled) was placed on a 300-mesh copper grid coated with carbon. Subsequently, the sample was dried and negatively stained by 2 wt.% uranyl acetate solution.

2.5. *In vitro* drug release studies

To investigate the *in vitro* release profile of PTX from HGC-PTX with 10 wt.% of PTX (HGC-PTX (10 wt.%)) and HO-GC-PTX with 20 wt.% of PTX (HO-GC-PTX (20 wt.%)) nanoparticles, we used 0.1 M sodium salicylate solution as the medium as reported previously [26]. The lyophilized HGC-PTX and HO-GC-PTX (1 mg) were dispersed in 1 mL of PBS, which was transferred to the cellulose ester membrane tube (molecular cutoff = 8000). The sample-containing tubes were immersed in PBS containing 0.1 M sodium salicylate and gently shaken at 37 °C in a water bath at 100 rpm. The medium was refreshed at various time intervals. The concentration of PTX was determined by HPLC analysis as described earlier [17].

2.6. Cytotoxicity of HO-GC-PTX nanoparticles

MDA-MB231 human breast cancer cells, obtained from the American Type Culture Collection (Rockville, MD), were cultured in RPMI 1640 (Gibco, Grand Island, NY) containing 10% (v/v) FBS (Gibco) and 1% (w/v) penicillin–streptomycin at 37 °C in a humidified 5% CO₂–95% air atmosphere. The cytotoxicity of free PTX, HGC, HO-GC, HGC-PTX, and HO-GC-PTX nanoparticles was evaluated using the MTT assay. Cells were seeded at a density of 1×10^4 cells/well in 96-well flat-bottomed plates, and allowed to adhere for overnight. The Cremophor-PTX stock solution (6 mg PTX/mL) was prepared by dissolving 200 µL of 12 mg/mL (14 mM) PTX in ethanol with an equal volume of Cremophor EL, followed by sonication for 30 min. The cells were washed twice with PBS and incubated for 2 days with various concentrations of Cremophor-based PTX, HGC, HO-GC, HGC-PTX, and HO-GC-PTX. The cells were then washed twice with PBS to eliminate the remaining drugs and fresh culture medium was added. Ten microliters of MTT solution (5 mg/mL in PBS) was added to each well and the cells were incubated further for 4 h at 37 °C. The media were removed and the cells were dissolved in DMSO. Absorbance at 570 nm was measured with a microplate reader (VERSAmax™, Molecular Devices Corp., Sunnyvale, CA).

2.7. Cellular uptake of HO-GC-PTX nanoparticles

Human HeLa H2B-GFP stable cell line was kindly provided by Korea Basic Science Institute, South Korea. The cell lines were cultured in Dulbecco's modified Eagle's medium, supplemented with 10% fetal bovine serum plus 5 mM L-glutamine and 5 µg/mL gentamicin, at 37 °C in a humidified 5% CO₂ incubator. The tested cells were seeded onto 35 mm coverglass bottom dishes and allowed to grow until a confluence of 70%. Prior to the experiment, cells were washed twice with PBS (pH 7.4) to remove the remnant growth medium, and then incubated for the desired time in serum-free medium containing HGC-PTX (10 wt.%) nanoparticles and HO-GC-PTX (20 wt.%) nanoparticles. The cells were then washed twice with ice-cold PBS (pH 7.4), fixed with fresh 4% paraformaldehyde for 3 min at room temperature, and mounted with Fluoromount-G™ (SouthernBiotech, Birmingham,

AL). The intracellular localization of Cy5.5 labeled HGC-PTX (10 wt.%) and HO-GC-PTX (20 wt.%) nanoparticles was visualized using a confocal laser scanning microscope (CLSM; LSM 510 Meta, Carl Zeiss Inc., Thornwood, NY) equipped with Argon (488 nm) and HeNe (543 nm) lasers for fluorescence. Images were acquired by multi-tracking to avoid bleed-through between the fluorophores and image analysis was carried out using LSM 510 software.

2.8. *In vivo* biodistribution of HO-GC-PTX nanoparticles

Athymic nude mice (20 g, Institute of Medical Science, Tokyo) were used for *in vivo* imaging experiment. Subcutaneous tumor models were established by inoculating 1.0×10^6 squamous cell carcinoma (SCC7) cells into the dorsal side of mice. When tumors grew to approximately 200 ± 30 mm³ in volume, saline (100 µL) and Cy5.5-labeled HO-GC-PTX (20 wt.%) (5 mg/kg in 100 µL of saline) were intravenously injected via the tail vein into SCC7 tumor-bearing mice. After injection of samples, the time-dependent *in vivo* biodistribution and tumor specificity of HO-GC-PTX (20 wt.%) were non-invasively imaged using the eXplore Optix System (Advanced Research Technologies Inc., Montreal, Canada) [22]. For the imaging study, laser power, exposure time and count time setting were optimized at 25 µW and 0.3 s per point. Near-infrared fluorescence (NIRF) emission (600–700 nm) was detected with a fast photomultiplier tube (Hamamatsu, Japan) and a time-correlated single photon counting system (Becker and Hickl GmbH, Berlin, Germany). The tumor specificity of HO-GC-PTX was quantitatively observed by measuring the NIR fluorescence intensity of tumor site, compared to normal tissues. All data are calculated using the region-of-interest (ROS) function of Analysis Workstation software (ART Advanced Research Technologies Inc., Montreal, Canada) and data are given as mean \pm s.e. for a group of three animals.

To give substantial evidence of tumor specificity of HO-GC-PTX, the mice were sacrificed at 3 days after injection of the sample, and major organs (livers, lungs, spleens, kidneys, and hearts) and tumors were excised. The NIRF signal intensity in different tissues were measured and imaged using a 12-bit CCD camera (Imaging Station 4000 MM; Kodak, New Haven, CT) equipped with a Cy5.5 emission filter sets (600 to 700 nm; Omega Optical). A quantification of *in vivo* tumor specificity of HO-GC-PTX was measured as total photons per centimeter squared per steradian (p/s/cm²/sr) per each tumor ($n = 3$ mice per group).

3. Results and discussion

3.1. Synthesis of HO-GC conjugates

Since DENA has been demonstrated as the effective hydrotropic agent for dissolution of PTX, we have attempted to prepare DENA-based hydrophobic oligomer terminated with carboxylic acid. Such oligomer would be useful as the hydrophobic moiety of amphiphilic GC because it may allow formation of self-assembled nanoparticles that can encapsulate large amount of PTX. In order to prepare the DENA-based oligomer, VBODENA monomer containing the vinyl group was first synthesized from 2-hydroxy nicotinic acid [16,17]. Oligo(VBODENA)-COOH ($M_n = 3520.43$ Da) was synthesized from the VBODENA monomer by free radical chain transfer polymerization in the presence of MPA as functional chain transfer agent and AIBN as an initiator (Fig. 1). MPA has been widely used as chain transfer agent, for various monomers, to obtain oligomers with controlled molecular weight and narrow polydispersity [27]. The other significant advantage of MPA as the chain transfer agent is generation of reactive carboxylic acid group at the end of the oligomeric chain, which could be used for further conjugation. The chemical structure and number-average molecular weight of VBODENA oligomer were obtained from the integration ratio of two methyl peaks of VBODENA (at 0.89 and

1.04 ppm) to the methylene peak of the MPA moiety (at 2.82 ppm) in ^1H NMR spectrum (see [Supplementary information, Fig. S1](#)).

The HO-GC conjugate was synthesized by chemical conjugation of the carboxylic group of VBODENA oligomer to the amine group of GC in the presence of EDAC and HOBt. The formation of the amide linkage was readily achieved by the reaction of the HOBt-activated ester with the amine group of GC, as demonstrated by the ^1H NMR spectrum (see [Supplementary information, Fig. S2](#)). The degree of substitution, defined as the number of oligomer per 100 sugar residues, was estimated to be 4.5% which could be characterized by the peak integration ratio of methyl groups of VBODENA (at 1.00 ppm and 1.20 ppm) to the characteristic peaks of GC. According to the ^1H NMR results, the weight percentage of hydrotropic oligomer in the HO-GC conjugate was 36.4%.

3.2. Preparation of HO-GC nanoparticles in aqueous conditions

The amphiphilic HO-GC conjugates formed nanoparticles spontaneously in an aqueous solution (PBS or distilled water) and their mean diameter was 313 nm ([Fig. 2a](#)), confirmed by using dynamic light scattering. The average size of nanoparticles was not significantly dependent on their concentrations (in the range of 1–5 wt.%), indicating that no inter-particular aggregation occurred. In addition, the mean diameter of nanoparticles was not remarkably changed for 50 days, and no precipitates were found in the solution ([Fig. 2b](#) and [c](#)). These results suggested that hydrotropic DENA oligomers in the nanoparticle play a role as the stable, hydrophobic inner cores. The critical aggregation concentration (cac) of HO-GC nanoparticles, determined using fluorescence spectroscopy, was 0.041 mg/mL, which was much lower than those of the conventional surfactants such as sodium dodecyl sulfate in water (2.3 mg/mL) [28]. These stable HO-GC nanoparticles with lower cac value may maintain their structural stability even at the dilute physiological condition in the body. [Fig. 2d](#) shows the cytotoxicity of HGC and HO-GC nanoparticles. Most of cells were viable in the presence of HGC and HO-GC nanoparticles at the concentrations applied in this study (0.1–50 mg/mL). This is in a good

agreement with the previous studies that biocompatible glycol chitosan nanoparticles showed excellent cell viability in the cell culture system [18,29]. The mean values of cell viability for HO-GC were slightly lower than that for HGC at high concentrations (>0.5 mg/mL). However, the differences between HGC and HO-GC nanoparticles were not statistically significant ($p > 0.05$).

3.3. Preparation of HO-GC-PTX nanoparticles

The hydrophobic PTX was easily encapsulated into HO-GC nanoparticles by a simple dialysis method [18]. The overall characteristics of HO-GC-PTX nanoparticles, including drug-loading content, drug-loading efficiency, and their respective mean diameters are summarized in [Table 1](#).

In order to determine the maximum loading capacity, we have varied the feed weight ratio of PTX to HGC and HO-GC nanoparticles from 10 wt.% to 30 wt.%. It should be emphasized that HO-GC nanoparticles could encapsulate significant amount of drug as much as 23.9 wt.%, which is significantly greater than other polysaccharide-based amphiphiles and HGC nanoparticles [18,30,31]. In particular, the maximum drug-loading amount of PTX in HO-GC nanoparticles was approximately 1.83-folds higher than that in HGC nanoparticles, when the feed ratio of PTX was 30 wt.% ([Table 1](#)). This higher loading drug efficiency of the HO-GC-PTX nanoparticles was obviously attributed to the presence of hydrotropic inner cores. However, when the feed amount of PTX increased above 30 wt.%, a substantial decrease in the drug-loading efficiency (less than 80%) was found. The mean diameter of HO-GC-PTX nanoparticles was in the range of 331–363 nm, which was smaller than that of HGC-PTX nanoparticles. This indicates that HO-GC-PTX formed more compact PTX-encapsulated nanoparticles.

3.4. Stability of HO-GC-PTX nanoparticles

[Fig. 3a](#) shows the photographs of the HGC-PTX and HO-GC-PTX solutions stored in PBS at 37 °C for 3 h, wherein different amounts of

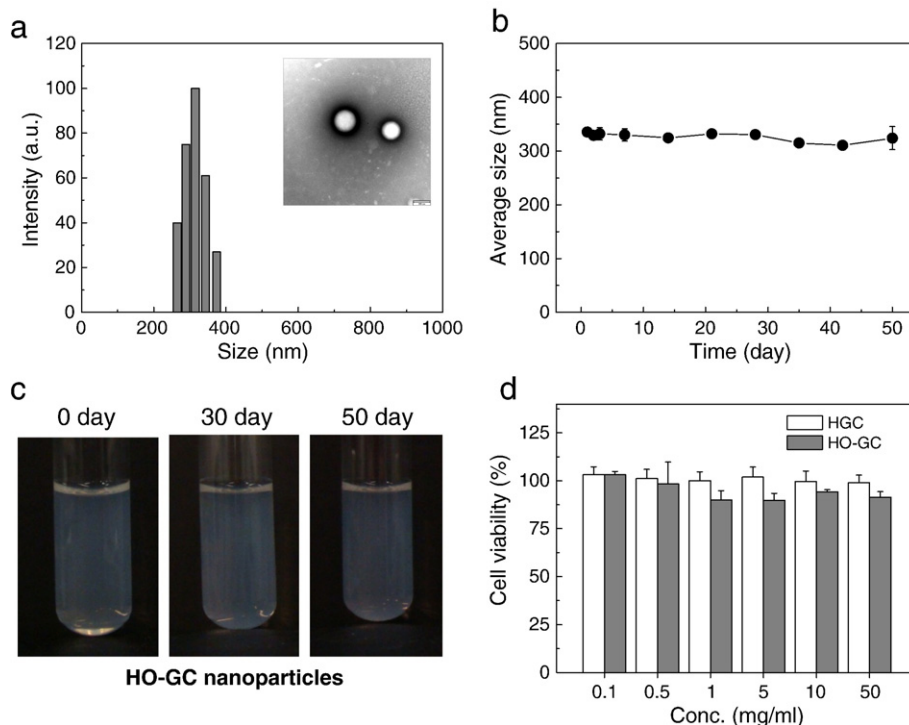


Fig. 2. *In vitro* characteristics of HO-GC nanoparticles. (a) Average size of HO-GC nanoparticles (1 mg/mL in PBS at 37 °C) was measured using dynamic light scattering. Inset image indicated TEM image of HO-GC nanoparticles in distilled water (1 mg/mL). (b) Particle size of HO-GC nanoparticles at 37 °C in PBS as a function of time. (c) Photographs of HO-GC solutions stored in PBS for up to 50 days. (d) Cytotoxicity of HGC and HO-GC nanoparticle. Cell viability of each sample was measured using MTT assay. Data represents mean \pm s.e. ($n = 5$).

Table 1
Characteristics of PTX-loaded HGC and HO-GC nanoparticles.

Sample	Feed amount of PTX (mg)	Loading content of PTX ^a (wt.%)	Loading efficiency ^b (%)	Size ^c (nm)
HGC	–	–	–	232 ± 13
HGC-PTX (10 wt.%)	10	9.2 ± 0.3	92.0 ± 3.0	372 ± 23
HGC-PTX (20 wt.%)	20	11.7 ± 0.2	58.5 ± 2.0	385 ± 43
HGC-PTX (30 wt.%)	30	13.0 ± 0.3	43.3 ± 3.0	400 ± 34
HO-GC	–	–	–	313 ± 20
HO-GC-PTX (10 wt.%)	10	9.8 ± 0.2	98.0 ± 2.0	331 ± 25
HO-GC-PTX (20 wt.%)	20	18.9 ± 0.5	94.7 ± 5.0	354 ± 23
HO-GC-PTX (30 wt.%)	30	23.9 ± 0.3	79.7 ± 3.0	363 ± 32

^a Loading content of PTX in nanoparticles were measured using HPLC.

^b Loading efficiency of PTX in nanoparticles were calculated from the ratio of loading content of PTX/feed amount of PTX in the nanoparticles.

^c Average size of each nanoparticle (1 mg/mL in PBS at 37 °C) was measured using dynamic light scattering.

PTX were encapsulated into the 100 mg of HGC and HO-GC nanoparticles. In the case of HGC-PTX solutions, a large amount of precipitates were observed within 1 h at room temperature, when the feed ratio of PTX was higher than 20 mg. It means that PTX-encapsulated HGC nanoparticles with higher PTX loading content are not stable in PBS. It is also reported that current polymeric nanoparticles have poor physical stability when they encapsulated excess hydrophobic drugs, due to the thermodynamic instability of drug-encapsulated nanoparticles in aqueous conditions [17]. On the other hand, there are no large aggregates in all the HO-GC-PTX solutions in the PBS condition and all the particles are well dispersed in PBS up to 2 weeks, indicating the thermodynamic stability of PTX-encapsulated particles in the aqueous condition.

To test the stability of different nanoparticles in the severe condition, the sample was centrifuged at 500, 700, and 1000 rpm for 10 min (Fig. 3b). As expected, most particles in HGC-PTX (20 wt.% or 30 wt.%) solution were precipitated in the bottom after centrifugation at 1000 rpm for 10 min, indicating instability of HGC-PTX particles. Only HGC-PTX (10 wt.%) particles showed a high stability to centrifugation. This result supports that HGC nanoparticles can imbibe 10 wt.% of PTX into the hydrophobic inner cores of 5 β -cholic acid. Noticeably, HO-GC-PTX nanoparticles maintained their physical stability after the centrifugation at 1000 rpm for 10 min. Importantly, HO-GC-PTX (20 wt.%) showed the maximum drug-loading efficacy of 94.7% and they were very stable in aqueous condition. Therefore, HO-GC-PTX (20 wt.%) nanoparticles were selected as a candidate for the next experiments. The poor physical stability of PTX-encapsulated nanoparticles could be surmounted by introducing hydrotropic oligomers into the glycol chitosan.

3.5. Characterizations of HO-GC-PTX nanoparticles *in vitro*

The average size of HO-GC-PTX nanoparticles was about 354 nm with a narrow size distribution and they were spherical in shape (Fig. 4a). HO-GC-PTX nanoparticles were also able to maintain their mean diameter for at least 2 weeks without aggregation (Fig. 4b). For *in vitro* release studies of sparingly water-soluble drugs like PTX, the selection of the medium is important because such drugs are not readily released in the absence of detergents or organic solvents. However, conventional detergents or organic solvents often disintegrate the self-assembled nanoparticles, which may affect release profile of PTX. In the previous study, sodium salicylate was successfully used as the hydrotropic agent to induce the release of PTX from the micelles [26]. To know the effect of sodium salicylate on the nanoparticle stability, the size of the nanoparticles at various concentrations of sodium salicylate was tested. As a consequence, it was found that no significant change in the size of nanoparticles occurred when sodium salicylate concentration was less than 0.1 M. Fig. 4c shows the release profile of PTX in PBS with 0.1 M sodium salicylate.

PTX was rapidly released for initial 12 h, and the release rate gradually decreased. More than 80% of PTX in the nanoparticles were released for 3 days. This release pattern of PTX from HO-GC nanoparticles was similar to that of HGC-PTX (10 wt.%) nanoparticles, as shown in Fig. 4c.

Cytotoxicity of free PTX dissolved in Cremophor EL/ethanol mixture (50 vol.%/50 vol.%), HGC-PTX (10 wt.%), and HO-GC-PTX (20 wt.%) nanoparticles in PBS were evaluated by determining their effects on viability of MDA-MB231 human breast cancer cells (Fig. 4d). All the samples showed cytotoxicity which was enhanced as the drug concentration increased. When the PTX concentration was higher than 0.5 μ g/mL, cytotoxicities of HO-GC-PTX and HGC-PTX were significantly lower than that free PTX formulation. In fact, less than 40% of the MDA-MB231 cells were viable after a 2-day exposure to 5 μ g/mL of PTX in Cremophor EL/ethanol formulation, whereas more than 80% of the cells survived under same concentration of PTX in the nanoparticles. This result indicated that nanoparticle formulation greatly reduced the cytotoxicity of the Cremophor EL/ethanol mixture in the free PTX formulation in the cell culture system [18].

The cellular uptake of Cy5.5-labeled HO-GC-PTX (20 wt.%) nanoparticles was observed using the confocal laser microscopy, in which the PTX concentration was fixed at 10 μ g/mL (Fig. 4e). Both of Cy5.5 labeled HO-GC-PTX (20 wt.%) and HGC-PTX (10 wt.%) nanoparticles (red colors) were readily taken up by the cells, which might be primarily due to the positively charged surface of glycol chitosan. It has been already reported that the higher binding affinity of the glycol chitosan nanoparticles at the cellular membrane may account for their facile internalization [32]. HGC-PTX (10 wt.%) nanoparticles presented a stronger fluorescence signal in the cell culture system,

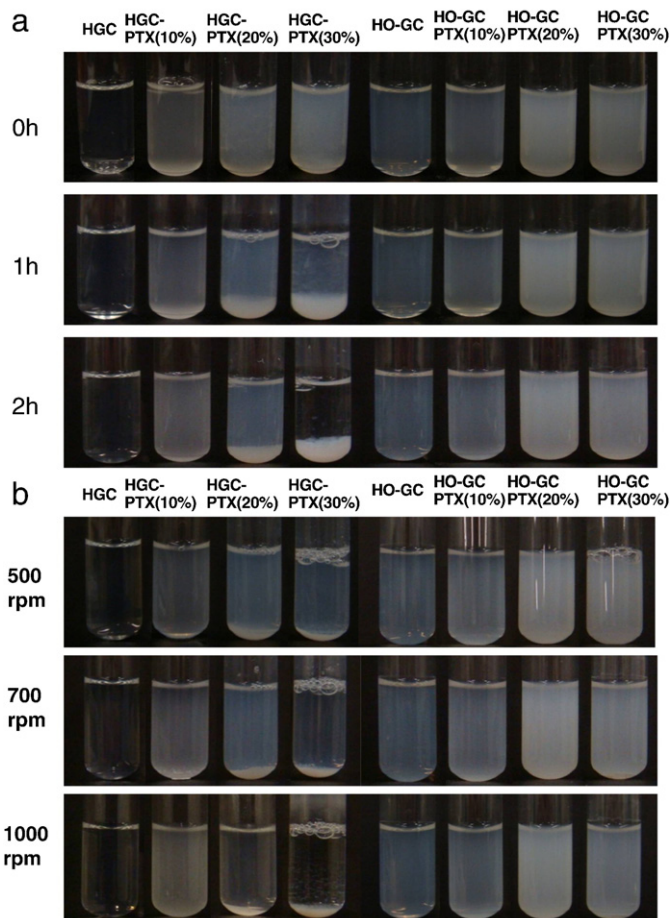


Fig. 3. Photographs of HGC-PTX and HO-GC-PTX nanoparticles in PBS as a function of (a) time and (b) centrifugation speed at 500 rpm, 700 rpm and 1000 rpm.

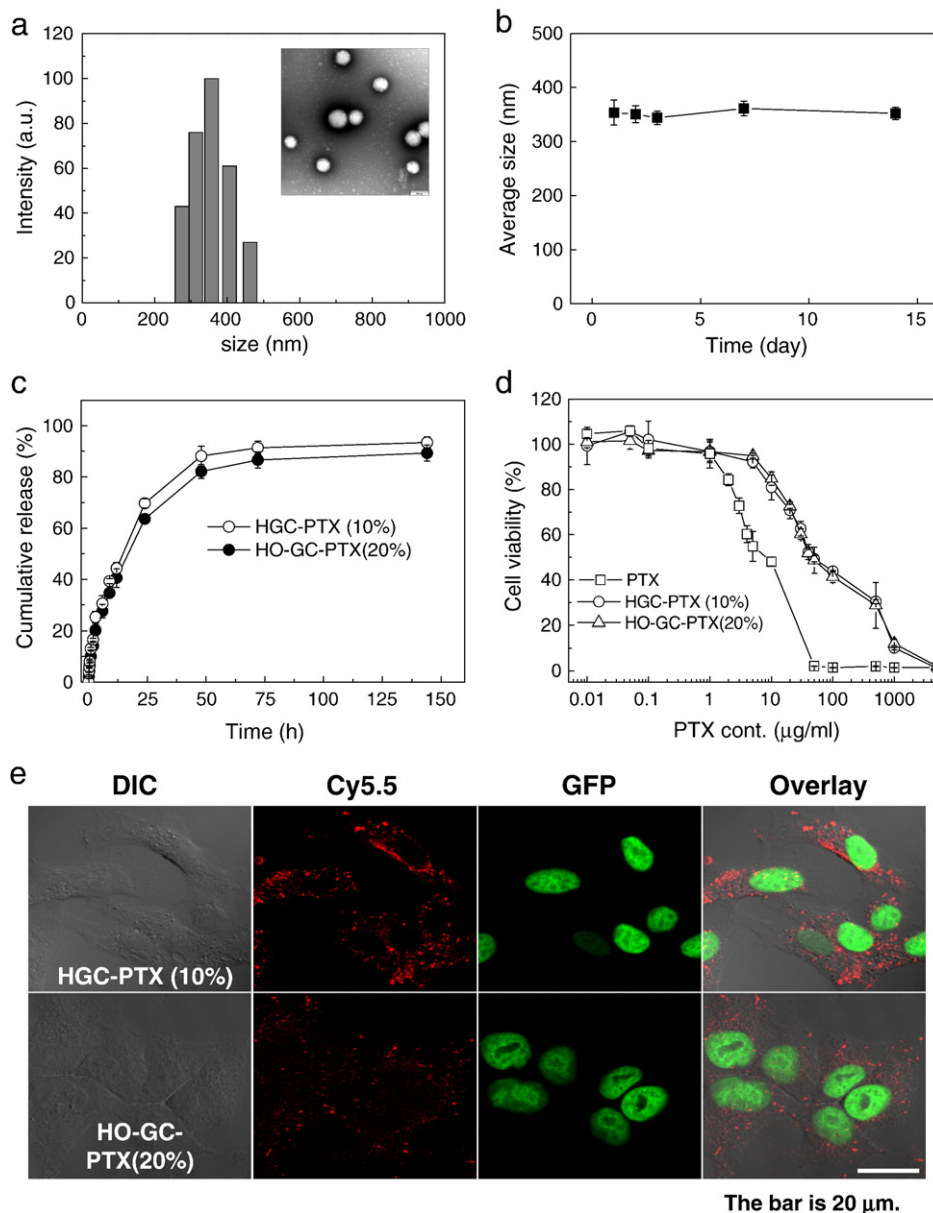


Fig. 4. (a) Average size of HO-GC-PTX (20 wt.%) nanoparticles (1 mg/mL in PBS at 37 °C) was measured using dynamic light scattering. Inset image indicated TEM image of HO-GC-PTX (20 wt.%) nanoparticles in distilled water (1 mg/mL). (b) Particle size of HO-GC-PTX (20 wt.%) nanoparticles at 37 °C in PBS as a function of time. Data represents mean \pm s.d. ($n = 5$). (c) PTX release profile from nanoparticles at 37 °C in PBS containing 0.1 M sodium salicylate. Data represents mean \pm s.d. ($n = 5$). (d) Cytotoxicity of HGC-PTX (10 wt.%) and HO-GC-PTX (20 wt.%) nanoparticles. Cell viability of each sample was measured using MTT assay. Data represents mean \pm s.d. ($n = 5$). (e) Cellular uptake characteristics of Cy5.5-labeled HGC-PTX (10 wt.%) and HO-GC-PTX (20 wt.%) nanoparticles in a cell culture system. Each nanoparticle containing 10 μg of PTX was incubated with HeLa H2B-GFP cells in culture media for 1 h (original magnification, $\times 400$).

compared to the signal by the HO-GC-PTX (20 wt.%). This is because HO-GC-PTX (20 wt.%) nanoparticles had smaller amount of Cy5.5-labeled glycol chitosan polymers at the same PTX concentration, compared to HGC-PTX (10 wt.%) nanoparticles. Furthermore, after 1 h incubation, PTX-encapsulated HGC or HO-GC particles were evenly dispersed in the cytoplasm parts, not in the nucleus part (green color). This result may imply that HO-GC-PTX nanoparticles with a higher drug-loading content can internalize the tumor cells and they dump the higher amount of PTX in the cytoplasm to induce successful tumor cell death.

3.6. *In vivo* biodistribution of HO-GC-PTX nanoparticles

In order to observe *in vivo* biodistribution of HO-GC-PTX (20 wt.%) nanoparticles, Cy5.5-labeled HO-GC-PTX nanoparticles (5 mg/kg in

100 μL of saline) were intravenously into SCC7 tumor-bearing mice and time-dependant biodistribution was observed using non-invasive NIRF imaging in live animals (Fig. 5a). After i.v. injection, a strong NIRF signal was observed in the whole body within 1 h post-injection, indicating the rapid circulation of nanoparticles in the blood stream. The strong fluorescence signal maintained up to 1 days, due to the prolonged circulation characteristics of glycol chitosan nanoparticles, compared to saline-treated mice [33]. Within 6 h post-injection, the nanoparticles are primarily localized at the liver tissue, whereas some particles are accumulated in the tumor tissue (solid arrows indicate tumor tissue). The strong fluorescence signal in the liver and the whole body gradually decreased after 1 day.

Fig. 5b shows the tumor specificity of HO-GC-PTX nanoparticles, compared to saline-treated mice. It should be noted that we could delineate subcutaneous tumors from the surrounding background

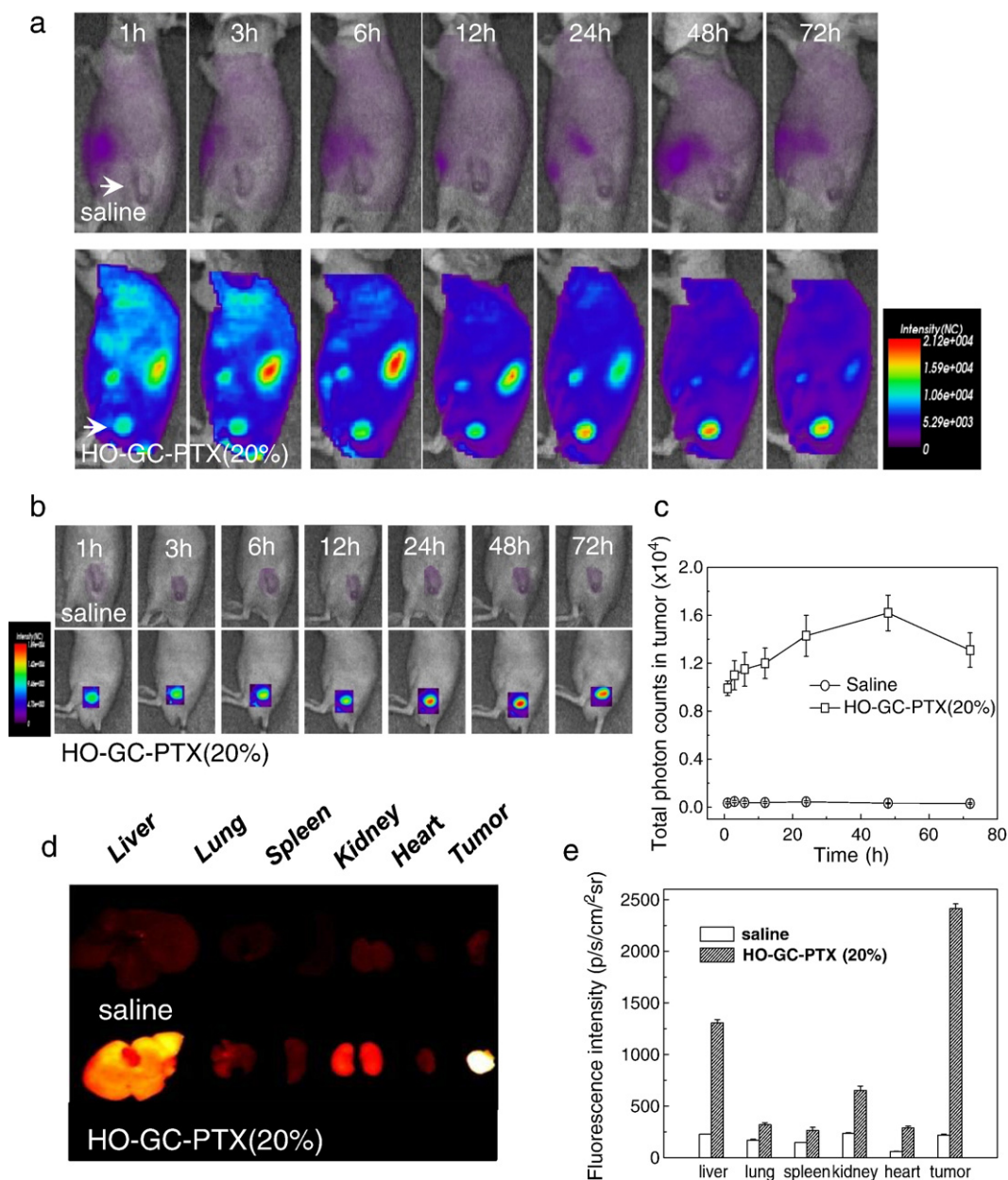


Fig. 5. (a) *In vivo* non-invasive NIRF images of time-dependent whole body imaging of SCC7 tumor-bearing mice after i.v. injection of saline and Cy5.5-labeled HO-GC-PTX (20 wt.%) (5 mg/kg). Solid arrow indicates the tumors. (b) *In vivo* tumor specificity of HO-GC-PTX (20 wt.%). (c) The total NIRF photon counts per centimeter squared per steradian (p/s/cm²/sr) per each tumor ($n = 3$ mice per group) as a function of time. (d) *Ex vivo* images of normal organs (liver, lung, spleen, kidney and heart) and tumors excised at 3 days post-injection of saline and HO-GC-PTX (20 wt.%) nanoparticles. (e) A quantification of *in vivo* biodistribution of HO-GC-PTX (20 wt.%) nanoparticles was recorded as total photon counts per centimeter squared per steradian (p/s/cm²/sr) per each excised organ at 3 days post-injection in SCC7 tumor-bearing mice ($n = 3$ mice per group). All data represent mean \pm s.e. ($n = 3$).

tissue after 1 h of injection. Furthermore, the NIRF signal in the tumor tissue gradually increased up to 2 days and maintained its strong signal up to 5 days, resulting from the tumor specificity of HO-GC-PTX nanoparticles. We already reported that stability and prolonged circulation profile of glycol chitosan nanoparticles resulted in an excellent tumor targeting ability in tumor-bearing mice [18–20,33]. The total photon counts of HO-GC-PTX nanoparticles in tumor tissue are 43.7-fold higher than that of saline-treated mice (Fig. 5c). To give substantial evidence of tumor specificity of HO-GC-PTX nanoparticles, major organs (liver, lung, spleen, kidney, heart, and tumor tissues) were isolated at 3 days post-injection and *ex vivo* images of each organ was observed (Fig. 5d). The strongest NIRF intensity was found on the tumor tissues. This indicated that HO-GC-PTX nanoparticles were predominantly accumulated in the tumor tissue, whereas some

particles are localized in liver and kidney. The fluorescence photon counts per gram from the tumor tissues were 1.8 to 8.4-fold higher than that of liver and spleen, respectively. These results suggest that HO-GC-PTX nanoparticles have a potential as a carrier for paclitaxel.

Polysaccharides (e.g., dextran, chitosan, pullulan, and hyaluronic acid) have been modified with hydrophobic moieties such as long alkyl chains and cholesteryl groups. They have widely studied as carriers for hydrophobic drug delivery. However, their therapeutic applications have been limited by poor drug-loading capacity, undesirable drug release kinetics, or the low stability. Hydrotropic agents have been used to increase the aqueous solubility of poorly soluble drugs. In the previous study, it was demonstrated that DENA-based hydrotropic micelles, PEG-*b*-PVBODENA, could accommodate PTX up to 37 wt.% with good stability [16]. In addition, DENA-based

polymeric hydrotropes exhibited enhanced solubilizing capacity than corresponding individual hydrotropic agent [34]. Our approach, in this study, was to develop glycol chitosan modified with the hydrotropic DENA-based oligomer as the potential carrier of PTX. The results showed that HO-GC were able to encapsulate PTX up to 23.9 wt.% with high drug-loading efficiency at about 80% (Table 1). It is interesting to note that such high PTX loading values with good loading efficiency have not been achieved with other amphiphilic chitosan derivatives. For example, the drug-loading efficiencies of alkyl chain-modified chitosan and bile acid-modified glycol chitosan decreased to 50–60%, when the loading content of the drug exceeds 10 wt.% [10,30,31]. Moreover, the stability of such nanoparticles became worse with increasing the loading content of the poorly soluble drugs. It is noteworthy to mention that the high loading capacity of HO-GC nanoparticles is due to the unique solubilizing property of hydrotropic DENA, which forms the inner cores of the nanoparticles, towards PTX.

4. Conclusion

In the present study, we have explored new hydrotropic oligomer-conjugated glycol chitosan (HO-GC) nanoparticles for solubilizing poorly water-soluble drug, PTX. The most significant feature of the present system is their hydrotropic inner cores, which can accommodate relatively large amount of PTX. HO-GC-PTX nanoparticles showed excellent thermodynamic stability in aqueous condition. Also, HO-GC-PTX nanoparticles presented a sustained drug release profile and rapid cellular uptake. Finally, biocompatible and stable PTX-encapsulated HO-GC nanoparticles had tumor specificity in the tumor-bearing mice. It could be concluded that the HO-GC has high potential as a new drug carrier of paclitaxel in cancer treatment.

Acknowledgements

This research was financially supported by the Real-Time Molecular Imaging Project, Global Research Laboratory of MEST, the Seoul R&DB program, the Korea Research Foundation (KRF-2006-311-D00075), and BioImaging Research Center at GIST.

Appendix A. Supplementary data

Supplementary data associated with this article can be found, in the online version, at doi:10.1016/j.jconrel.2009.06.015.

References

- [1] P.B. Myrdal, S.H. Yalkowsky, *Solubilization of Drugs in Aqueous Media*, Marcel Dekker, New York, 2002.
- [2] E.K. Rowinsky, R.C. Donehower, Paclitaxel (taxol), *N. Engl. J. Med.* 332 (15) (1995) 1004–1014.
- [3] A.K. Singla, A. Garg, D. Aggarwal, Paclitaxel and its formulations, *Int. J. Pharm.* 235 (1–2) (2002) 179–192.
- [4] V. Martin, Overview of paclitaxel (Taxol), *Semin. Oncol. Nurs.* 9 (4 Suppl 2) (1993) 2–5.
- [5] H. Gelderblom, J. Verweij, K. Nooter, A. Sparreboom, Cremophor EL: the drawbacks and advantages of vehicle selection for drug formulation, *Eur. J. Cancer* 37 (13) (2001) 1590–1598.
- [6] S. Mielke, A. Sparreboom, K. Mross, Peripheral neuropathy: a persisting challenge in paclitaxel-based regimens, *Eur. J. Cancer* 42 (1) (2006) 24–30.
- [7] D. Loven, H. Levavi, G. Sabach, R. Zart, M. Andras, A. Fishman, Y. Karmon, T. Levi, R. Dabby, N. Gadoth, Long-term glutamate supplementation failed to protect against peripheral neurotoxicity of paclitaxel, *Eur. J. Cancer Care* 18 (1) (2009) 78–83.
- [8] E. Lee, J. Lee, I.H. Lee, M. Yu, H. Kim, S.Y. Chae, S. Jon, Conjugated chitosan as a novel platform for oral delivery of paclitaxel, *J. Med. Chem.* 51 (20) (2008) 6442–6449.
- [9] W. Bouquet, W. Ceelen, B. Fritzing, P. Pattyn, M. Peeters, J.P. Remon, C. Vervaet, Paclitaxel/beta-cyclodextrin complexes for hyperthermic peritoneal perfusion—formulation and stability, *Eur. J. Pharm. Biopharm.* 66 (3) (2007) 391–397.
- [10] J.H. Kim, Y.S. Kim, S. Kim, J.H. Park, K. Kim, K. Choi, H. Chung, S.Y. Jeong, R.W. Park, I.S. Kim, I.C. Kwon, Hydrophobically modified glycol chitosan nanoparticles as carriers for paclitaxel, *J. Control. Release* 111 (1–2) (2006) 228–234.
- [11] J.A. Zhang, G. Anyarambhatla, L. Ma, S. Ugwu, T. Xuan, T. Sardone, I. Ahmad, Development and characterization of a novel Cremophor EL free liposome-based paclitaxel (LEP-ETU) formulation, *Eur. J. Pharm. Biopharm.* 59 (1) (2005) 177–187.
- [12] T.Y. Kim, D.W. Kim, J.Y. Chung, S.G. Shin, S.C. Kim, D.S. Heo, N.K. Kim, Y.J. Bang, Phase I and pharmacokinetic study of Genexol-PM, a cremophor-free, polymeric micelle-formulated paclitaxel, in patients with advanced malignancies, *Clin. Cancer Res.* 10 (11) (2004) 3708–3716.
- [13] K. Holmberg, D.O. Shah, M.J. Schwuger, *Handbook of Applied Surface and Colloid Chemistry*, Wiley, Chichester, 2002.
- [14] A.A. Rasool, A.A. Hussain, L.W. Dittert, Solubility enhancement of some water-insoluble drugs in the presence of nicotinamide and related compounds, *J. Pharm. Sci.* 80 (4) (1991) 387–393.
- [15] J. Lee, S.C. Lee, G. Acharya, C.J. Chang, K. Park, Hydrotropic solubilization of paclitaxel: analysis of chemical structures for hydrotropic property, *Pharm. Res.* 20 (7) (2003) 1022–1030.
- [16] S.C. Lee, K.M. Huh, J. Lee, Y.W. Cho, R.E. Galinsky, K. Park, Hydrotropic polymeric micelles for enhanced paclitaxel solubility: *in vitro* and *in vivo* characterization, *Biomacromolecules* 8 (1) (2007) 202–208.
- [17] K.M. Huh, S.C. Lee, Y.W. Cho, J. Lee, J.H. Jeong, K. Park, Hydrotropic polymer micelle system for delivery of paclitaxel, *J. Control. Release* 101 (1–3) (2005) 59–68.
- [18] J.H. Kim, Y.S. Kim, K. Park, S. Lee, H.Y. Nam, K.H. Min, H.G. Jo, J.H. Park, K. Choi, S.Y. Jeong, R.W. Park, I.S. Kim, K. Kim, I.C. Kwon, Antitumor efficacy of cisplatin-loaded glycol chitosan nanoparticles in tumor-bearing mice, *J. Control. Release* 127 (1) (2008) 41–49.
- [19] K.H. Min, K. Park, Y.S. Kim, S.M. Bae, S. Lee, H.G. Jo, R.W. Park, I.S. Kim, S.Y. Jeong, K. Kim, I.C. Kwon, Hydrophobically modified glycol chitosan nanoparticles-encapsulated camptothecin enhance the drug stability and tumor targeting in cancer therapy, *J. Control. Release* 127 (3) (2008) 208–218.
- [20] H.Y. Hwang, I.S. Kim, I.C. Kwon, Y.H. Kim, Tumor targetability and antitumor effect of docetaxel-loaded hydrophobically modified glycol chitosan nanoparticles, *J. Control. Release* 128 (1) (2008) 23–31.
- [21] J. Hyung Park, S. Kwon, M. Lee, H. Chung, J.H. Kim, Y.S. Kim, R.W. Park, I.S. Kim, S. Bong Seo, I.C. Kwon, S. Young Jeong, Self-assembled nanoparticles based on glycol chitosan bearing hydrophobic moieties as carriers for doxorubicin: *in vivo* biodistribution and anti-tumor activity, *Biomaterials* 27 (1) (2006) 119–126.
- [22] J.H. Park, S. Kwon, J.O. Nam, R.W. Park, H. Chung, S.B. Seo, I.S. Kim, I.C. Kwon, S.Y. Jeong, Self-assembled nanoparticles based on glycol chitosan bearing 5beta-cholanic acid for RGD peptide delivery, *J. Control. Release* 95 (3) (2004) 579–588.
- [23] J.H. Kim, Y.S. Kim, K. Park, E. Kang, S. Lee, H.Y. Nam, K. Kim, J.H. Park, D.Y. Chi, R.W. Park, I.S. Kim, K. Choi, I. Chan Kwon, Self-assembled glycol chitosan nanoparticles for the sustained and prolonged delivery of antiangiogenic small peptide drugs in cancer therapy, *Biomaterials* 29 (12) (2008) 1920–1930.
- [24] H.S. Yoo, J.E. Lee, H. Chung, I.C. Kwon, S.Y. Jeong, Self-assembled nanoparticles containing hydrophobically modified glycol chitosan for gene delivery, *J. Control. Release* 103 (1) (2005) 235–243.
- [25] Y.J. Son, J.S. Jang, Y.W. Cho, H. Chung, R.W. Park, I.C. Kwon, I.S. Kim, J.Y. Park, S.B. Seo, C.R. Park, S.Y. Jeong, Biodistribution and anti-tumor efficacy of doxorubicin loaded glycol-chitosan nanoaggregates by EPR effect, *J. Control. Release* 91 (1–2) (2003) 135–145.
- [26] Y.W. Cho, J. Lee, S.C. Lee, K.M. Huh, K. Park, Hydrotropic agents for study of *in vitro* paclitaxel release from polymeric micelles, *J. Control. Release* 97 (2) (2004) 249–257.
- [27] A. Yamazaki, J.M. Song, F.M. Winnik, J.L. Brash, Synthesis and solution properties of fluorescently labeled amphiphilic (N-alkylacrylamide) oligomers, *Macromolecules* 31 (1) (1998) 109–115.
- [28] S. Kwon, J.H. Park, H. Chung, I.C. Kwon, S.Y. Jeong, Physicochemical characteristics of self-assembled nanoparticles based on glycol chitosan bearing 5b-cholanic acid, *Langmuir* 19 (24) (2003) 10188–10193.
- [29] K. Kim, S. Kwon, J.H. Park, H. Chung, S.Y. Jeong, I.C. Kwon, I.S. Kim, Physicochemical characterizations of self-assembled nanoparticles of glycol chitosan-deoxycholic acid conjugates, *Biomacromolecules* 6 (2) (2005) 1154–1158.
- [30] C. Zhang, P. Qineng, H. Zhang, Self-assembly and characterization of paclitaxel-loaded N-octyl-O-sulfate chitosan micellar system, *Colloids Surf., B Biointerfaces* 39 (1–2) (2004) 69–75.
- [31] J.M. Yu, Y.J. Li, L.Y. Qiu, Y. Jin, Self-aggregated nanoparticles of cholesterol-modified glycol chitosan conjugate: preparation, characterization, and preliminary assessment as a new drug delivery carrier, *Eur. Polym. J.* 44 (3) (2008) 555–565.
- [32] H.Y. Nam, S.M. Kwon, H. Chung, S.Y. Lee, S.H. Kwon, H. Jeon, Y. Kim, J.H. Park, J. Kim, S. Her, Y.K. Oh, I.C. Kwon, K. Kim, S.Y. Jeong, Cellular uptake mechanism and intracellular fate of hydrophobically modified glycol chitosan nanoparticles, *J. Control. Release* 135 (3) (2009) 259–267.
- [33] K. Park, J.H. Kim, Y.S. Nam, S. Lee, H.Y. Nam, K. Kim, J.H. Park, I.S. Kim, K. Choi, S.Y. Kim, I.C. Kwon, Effect of polymer molecular weight on the tumor-targeting characteristics of self-assembled glycol chitosan nanoparticles in tumor-bearing mice, *J. Control. Release* 112 (2007) 305–314.
- [34] S.C. Lee, G. Acharya, J. Lee, K. Park, Hydrotropic polymers: synthesis and characterization of polymers containing picolynicotinamide moieties, *Macromolecules* 36 (7) (2003) 2248–2255.